

BASIC SCIENCE ARTICLE OPEN



Severe intraventricular hemorrhage causes long-lasting structural damage in a preterm rabbit pup model

Olga Romantsik¹✉, Emily Ross-Munro², Susanne Grönlund¹, Bo Holmqvist³, Anders Brinte³, Erik Gerdtsen³, Suvi Vallius¹, Matteo Bruschetini¹, Xiaoyang Wang^{4,5}, Bobbi Fleiss^{2,6,7}✉ and David Ley^{1,7}

© The Author(s) 2022

BACKGROUND: Intraventricular hemorrhage causes significant lifelong mortality and morbidity, especially in preterm born infants. Progress in finding an effective therapy is stymied by a lack of preterm animal models with long-term follow-up. This study addresses this unmet need, using an established model of preterm rabbit IVH and analyzing outcomes out to 1 month of age. **METHODS:** Rabbit pups were delivered preterm and administered intraperitoneal injection of glycerol at 3 h of life and approximately 58% developed IVH. Neurobehavioral assessment was performed at 1 month of age followed by immunohistochemical labeling of epitopes for neurons, synapses, myelination, and interneurons, analyzed by means of digital quantitation and assessed via two-way ANOVA or Student's *t* test. **RESULTS:** IVH pups had globally reduced myelin content, an aberrant cortical myelination microstructure, and thinner upper cortical layers (I–III). We also observed a lower number of parvalbumin (PV)-positive interneurons in deeper cortical layers (IV–VI) in IVH animals and reduced numbers of neurons, synapses, and microglia. However, there were no discernable changes in behaviors. **CONCLUSIONS:** We have established in this preterm pup model that long-term changes after IVH include significant wide-ranging alterations to cortical organization and microstructure. Further work to improve the sensitivity of neurocognitive testing in this species at this age may be required.

Pediatric Research (2022) 92:403–414; <https://doi.org/10.1038/s41390-022-02075-y>

IMPACT:

- This study uses an established animal model of preterm birth, in which the rabbit pups are truly born preterm, with reduced organ maturation and deprivation of maternally supplied trophic factors.
- This is the first study in preterm rabbits that explores the impacts of severe intraventricular hemorrhage beyond 14 days, out to 1 month of age.
- Our finding of persisting but subtle global changes including brain white and gray matter will have impact on our understanding of the best path for therapy design and interventions.

INTRODUCTION

Intraventricular hemorrhage (IVH) occurs in up to 45% of preterm infants born below gestational age 26 weeks, with severe IVH (≥ 3 grade) occurring in nearly 30% of those very fragile infants.^{1–3} These numbers have increased as survival of the smallest infants, 22–23 weeks, improves.^{4,5} Of these infants with severe IVH (≥ 3 grade), up to 60% will go on to develop post-hemorrhagic ventricular dilation (PHVD).^{1,6} We have no treatments for IVH, and infants born preterm and affected by IVH have a higher risk for impaired neurodevelopment^{4,7,8} compared to their age-matched non-IVH affected peers and this is especially true for infants who go on to develop PHVD.^{9–14}

IVH arises in the germinal matrix, a layer of immature neuronal and glial precursors adjacent to the ependymal lining of the ventricles interwoven with a dense network of delicate blood vessels. These vessels have no structural support, and lack autoregulation, which makes them susceptible to fluctuations of vascular flow. The risk factors for IVH include immaturity (gestational age, birth weight), vascular fluctuations (hypotension, need for resuscitation), and inflammation (interleukin 1B polymorphism,¹⁵ and chorioamnionitis.¹⁶) The development of therapies for IVH-related brain injury is stymied by a lack of well-characterized representative animal models.

¹Department of Clinical Sciences Lund, Division of Pediatrics, Lund University, Skåne University Hospital, 21185 Lund, Sweden. ²School of Health and Biomedical Sciences, STEM College, RMIT University, Bundoora 3083 VIC, Australia. ³ImaGene-iT AB, 22363 Lund, Sweden. ⁴Centre of Perinatal Medicine & Health, Institute of Clinical Sciences, Department of Obstetrics and Gynecology, Sahlgrenska Academy, Gothenburg University, 40530 Gothenburg, Sweden. ⁵Henan Key Laboratory of Child Brain Injury and Pediatric Clinical Research Center, Institute of Neuroscience and Third Affiliated Hospital of Zhengzhou University, Zhengzhou, China. ⁶Université de Paris, NeuroDiderot, Inserm, 75019 Paris, France. ⁷These authors contributed equally: Fleiss Bobbi, Ley David. ✉email: olga.romantsik@med.lu.se; bobbi.fleiss@rmit.edu.au

Received: 2 December 2021 Revised: 10 March 2022 Accepted: 23 March 2022
Published online: 3 May 2022

Models of IVH across species have revealed mechanisms potentially involved in its pathophysiology, reviewed in ref.¹⁷ including the distribution of extracellular hemoglobin within white matter (WM), toxicity of blood product degradation, onset of neuroinflammation characterized by microglia and astrocyte activation and infiltration by systemic immune cells, the death of neuronal and glial cells, and arrest of pre-oligodendrocyte maturation. However, most IVH models utilize pups delivered at term with correspondingly mature physiology but with varying degrees of brain maturity when compared to the human infant, ranging from preterm (rodents) to term (piglets, dogs).^{17,18} The lack of preterm delivery in those models omits several important aspects of preterm birth, such as respiratory instability, immaturity of the coagulation system, a deficit of trophic factors, and the impact of hemorrhage into the immature brain parenchyma.¹⁷

One of the few small animal models of IVH that incorporates preterm birth is the preterm rabbit pup model,^{19–21} which is used in the current study. Preterm rabbit pups exhibit many aspects of prematurity relevant for human preterm infants, including smaller lungs with a reduced alveolar surface and lower expression of surfactant proteins,^{22,23} the propensity to development of necrotizing enterocolitis-like disease,²⁴ renal immaturity,²⁵ and reduced levels of trophic growth factors such as insulin-like growth factor-1.²⁶ The preterm rabbit brain development at post-conceptual day 29 arguably corresponds to brain development in humans at gestation week 24–25,^{20,27,28} the period of peak vulnerability to IVH.

Across all models of IVH, most studies report on short-term outcomes (<14 days), and there is a lack of neurobehavioral testing in preterm models. Thus, to fill this gap in our knowledge, we aimed to use our established model of IVH in preterm rabbit pups and characterize out to 1 month of age (equivalent to a 1-year-old human) survival, neurobehaviors, neuropathology, and cortical development.

MATERIALS AND METHODS

Animals

The study was approved by the Swedish Animal Ethics Committee in Lund (dnr. M 2-16). We used the preterm rabbit pup model of glycerol-induced IVH as previously described.^{20,21} Seventy-seven preterm rabbit pups of both sexes from 12 different litters were included in the study. Detailed methods can be found in the Supplementary Methods. A half-breed between the New Zealand White and Lop was used (Christer Månsson, Löberöd, Sweden). Pups were delivered via cesarean section at post-conceptual day 29 (term = 32 days). At 3 h of age, all pups received intraperitoneal (i.p.) injection of 50% (v/v) sterile glycerol (6.5 g/kg; Teknova, Hollister, CA) to induce IVH. Thereafter, pups were randomly allocated (<https://www.random.org/>) to a wet-nurse doe for the remainder of the experiment. The study endpoint was PND33, which corresponds roughly to brain development of a year-old toddler.²⁹

IVH and PHVD detection

The presence and severity of IVH were evaluated by high-frequency ultrasound (HFU) (VisualSonics Vevo 2100, VisualSonics Inc., ON, Canada) using an MS-550D 40 MHz transducer at PND1 and PND2. Pups with IVH (any grade) as determined by HFU (HFU was done by O.R.) were assigned to the IVH group and those without detectable IVH were used as controls. To confirm the presence of PHVD, an *ex vivo* brain HFU was also performed directly after termination via an artificial ultrasound window created by shaving the skull and making a short skin mid-sagittal incision and making a careful osteotomy (approximately 3 mm), taking care to prevent damage to the underlying dura. The obtained calvarial opening was irrigated with sterile saline to wash out tissue microparticles.

Sex determination

To detect the male sex, polymerase chain reaction for the detection of SRY (specific region of the Y chromosome) sequences was used; details of the PCR conditions and the primer sequences are found in the Supplementary Methods.

Neurobehavioral examination

Neurobehavioral testing was performed between PND29 and 32 as previously described^{20,30,31} by an investigator blinded to the group of the pup. There was no visible differences in general animal performance that allowed us to discriminate between the groups. The motor examination included muscle tone and strength, gait, and righting reflex. The neurocognitive testing included open field (OF) test and the object recognition test (ORT). The ORT included a familiarization phase and a trial phase, which was spaced by an interest interval of 5-, 30-, and 240-min on testing days 2, 3, and 4, respectively. The specific details of the tests, arena, and the paradigms in full are found in the Supplementary Methods section. The room temperature was set at 21 °C and works undertaken as previously in rabbit pups at earlier time points.^{31,32} Data were analyzed with the Video Tracking Software (SMART, Panlab SL, Barcelona, Spain). The authors were blinded to animal group assignment throughout testing, data gathering, and analysis.

Tissue collection

Tissues were collected and processed as previously³¹ and as described in detail in the Supplementary Methods. In brief, brains were transcardially perfused and then post-fixed for 24 h in 4% paraformaldehyde before being processed to paraffin and cut at 5 µm.

Immunohistochemistry (IHC)

Sections were prepared and stained using well-established protocols as previously³¹ and described in detail in the Supplementary Methods. In brief, sections were rehydrated and antigen retrieval was performed with citrate buffer, pH 6 + 0.04% Tween 20, at 95 °C for 20 min followed by blocking with 0.1 M phosphate-buffered saline (PBS) containing 0.05% Triton X-100 (TX) and 1% bovine serum albumin (PBS-BSA-TX) for 30 min and then the application of primary antibodies listed in Table 1 diluted in PBS-BSA-TX and applied for 16 h, at 4 °C in a humidified chamber: As antibody specificity controls, in adjacent sections the primary antibody incubation was excluded. Sections were then incubated with horseradish peroxidase (HRP)-conjugated secondary antibodies, see Table 1, for 30 min at room temperature and diaminobenzidine (DAB, 0.5 mg/ml) plus hydrogen peroxidase (0.1%) for 10 min at room temperature to reveal the antigen–antibody binding. Sections were dehydrated and coverslipped in Pertex (Histolab, Gothenburg, Sweden).

Immunofluorescence (IF)

A standardized IF protocol was conducted as previously described³³ and described in detail in the Supplementary Methods, including no primary antibody controls. In brief, slides were rehydrated and antigens were retrieved with citrate buffer (10 mM, pH 6.0) at 95 °C for 20 min. Sections were then exposed for 20 min to a 0.1% Sudan Black block diluted in 70% EtOH, as previously,³⁴ and then blocked further in 5% normal goat serum 0.2% Triton X-100 for 1 h at room temperature. Slides were incubated in humidified chambers overnight at 4 °C with the primary antibodies and then the secondary antibodies listed in Table 1. Sections were then stained with 4,6-diamidino-2-phenylindole and coverslipped.

Image acquisition and quantification

We initially verified that there was no labeling in the antibody-omitted specificity control sections. Analyses were conducted by investigators blinded to the treatment groups. Full details of the methods can be found in the Supplementary Methods section. Sections were scanned to obtain digital images and the region of interest (ROI) extracted with resolution of scale fixed across sections, regions, and analysis.

NeuN-positive cells were calculated with Fiji by the default auto-threshold segmentation method and watershed separation following primary smoothing or were manually counted if the separation of cells was not achieved. The number of identified cells was divided by the whole area for neuron density assessment.

The area coverage for glial fibrillary acid protein (GFAP), synaptophysin, and myelin basic protein (MBP) labeling was calculated using a fixed threshold (relative to background) and the relative area (positive area/overall area) was calculated.

Directionality and organization of the MBP staining was analyzed using Fiji (<https://doi.org/10.1088/1758-5090/aa6204>). MBP was assessed in the middle third of a fixed-width image of the cortical plate to focus on the region with the greatest number of ascending fibers.

Table 1. Antibodies used in the study.

| Antigen | Species and antibody type | Product identifier |
|--|--|--|
| Immunohistochemistry | | |
| Neuronal nuclear antigen (NeuN) | Mouse monoclonal (1:100) | MAB377, Millipore, Terrecula, CA, USA |
| Synaptophysin | Mouse monoclonal (1:40) | Clone Sy38, ab8049, Abcam, Cambridge, UK |
| Myelin basic protein (MBP) | Mouse monoclonal (1:50) | Clone SMI94, 836504, BioLegend, San Diego, CA, USA |
| Ionized calcium-binding adapter molecule 1 (IBA 1) | Rabbit polyclonal (1:1000) | 019-19741, FUJIFILM Wako, Japan |
| Glial fibrillary acid protein (GFAP) | Chicken polyclonal (1:750) | ab4674, Abcam, Cambridge, UK |
| Mouse IgG | Goat polyclonal (1:1) | MP-7452, Vector Oxfordshire, UK |
| Chicken IgY | Donkey polyclonal (1:500) | 703-585-155 Jackson IR, West Grove PA, USA |
| Immunofluorescence | | |
| Chicken ovalbumin upstream promoter transcription factor-interacting protein 2 (CTIP2) | Rat monoclonal (1:500) | ab18465, Abcam, VIC, Australia |
| N-terminal EF-hand calcium binding protein 1 (NECAB1) | Mouse polyclonal (1:500) | PA5-54849, Thermo Fisher, VIC, Australia |
| Parvalbumin (PV) | Mouse monoclonal (1:250) | PV235, Swant, Burgdorf, Switzerland |
| Perineuronal net acetylgalactosamines | Wisteria Floribunda lectin (WFL, non-antibody based) (1:500) | B-1355, Vector laboratories via Abacus, QLD, Australia |
| Anti-mouse IgG | 594 goat polyclonal (1:200) | A11034, Thermo Fisher, VIC, Australia |
| Biotin | Streptavidin 488 conjugate (1:1000) | S11223, Thermo Fisher, VIC, Australia |
| Anti-rat IgG | 594 goat polyclonal (1:500) | A11007, Thermo Fisher, VIC, Australia |
| Anti-mouse IgG | 594 goat polyclonal (1:500) | A11011, Thermo Fisher, VIC, Australia |

For interneuron analysis, upper and lower cortical regions were defined as layers I–III and IV–VI, respectively, as described previously.³³ Immunoreactive cells were counted manually by a blinded observer using the CellSens Dimension counter tool. PV+ cells were identified as having a defined cell body within the section, and WFL+PNN+ were defined as an entire halo encompassing a PV+ interneuron.

The mean of the left and right regions for each analysis and ROI was used for statistical analysis.

Statistical analysis

Kaplan–Meier curve with a Gehan–Breslow–Wilcoxon test was used for survival analysis. For neurobehavioral testing, a one-tailed *T* test was employed based on the expected direction of change from previous studies,^{1,2} and analyses were performed using SPSS (PASW Statistics 18, IBM, Deutschland GmbH).

For cortical layering analysis, an unpaired Student's *t* test assessed treatment (presence of IVH) vs control effect on total cortical depth (Layers I–VI). Grouped data of layer depth (I–III, VI, V–VI; IVH vs control) and comparisons across regions for staining of cell types with IHC were analyzed using two-way analysis of variance (ANOVA), and when statistical significance was attained for treatment (presence of IVH) vs control (no IVH), post hoc analysis was performed with Sidak's multiple comparison using $\alpha = 0.05$. For IHC analyses, including cortical layers, perineuronal net (PNN), interneuron, and myelin, organization statistics were undertaken with GraphPad Prism (9.0, San Diego, CA) and post hoc analysis was also performed with Sidak's multiple comparison using $\alpha = 0.05$. Results are shown as mean (standard deviation) or median (interquartile range or confidence interval 95%). For all analyses, $p < 0.05$ was indicative of statistical significance.

RESULTS

As summarized in Fig. 1a, 77 preterm rabbit pups (female = 27, male = 45, unknown = 5) from 12 litters were included in this study who were cross-fostered to a total of ten wet nurses. In total, 88 pups were delivered, but 4 were born dead and 7 died between birth and before 3 h of age when glycerol was

administered. All pups received glycerol and 58% developed IVH as assessed with ultrasound. Twenty-one preterm pups (=27%) survived to the endpoint of the study (PND33). Of those 21 preterm pups, 8 (=38%) (females = 2) had IVH and developed PHVD and 13 (=62%) (females = 2) were used as controls (Fig. 1a). Following termination of the pups at PND33, we confirmed the development of various degrees of PHVD in all 8 animals in the IVH group (examples in Fig. 1b–d). One pup in the IVH group had a considerably milder PHVD and was therefore excluded from all subsequent analyses; this pup was male and had otherwise regular post-natal growth. All 13 animals in the control group had a normal brain ultrasound finding (representative images in Fig. 1b).

Pups with IVH had reduced survival rates

There were no differences in birth weight, bi-parietal measurement at birth, and in postnatal growth between the groups (Fig. 2a, b) or by sex for each treatment (data not shown due to small *n*). Survival was drastically diminished in pups with IVH compared to the controls (17.8 vs 40.6 %, $p = 0.004$, Gehan–Breslow–Wilcoxon test; Fig. 2c). Survival in female pups (control and IVH) was significantly lower compared to male pups (control and IVH) ($p = 0.044$, Gehan–Breslow–Wilcoxon test; Fig. 2d). Fewer female preterm pups with IVH survived until the study endpoint compared to the preterm male pups ($p = 0.013$; Fig. 2d).

IVH had no impact on the assessed neurodevelopmental tests

At PND 29–32, all surviving preterm pups in both IVH and control groups were exposed to neurobehavioral assessment. It was impossible to distinguish phenotypically the preterm pups with IVH/PHVD from the controls: all the surviving pups managed to feed independently, moved freely within the cages, and exhibited no differences when assessed for muscle tone and righting reflex (data not shown). The gait and coordination examination on a 60°

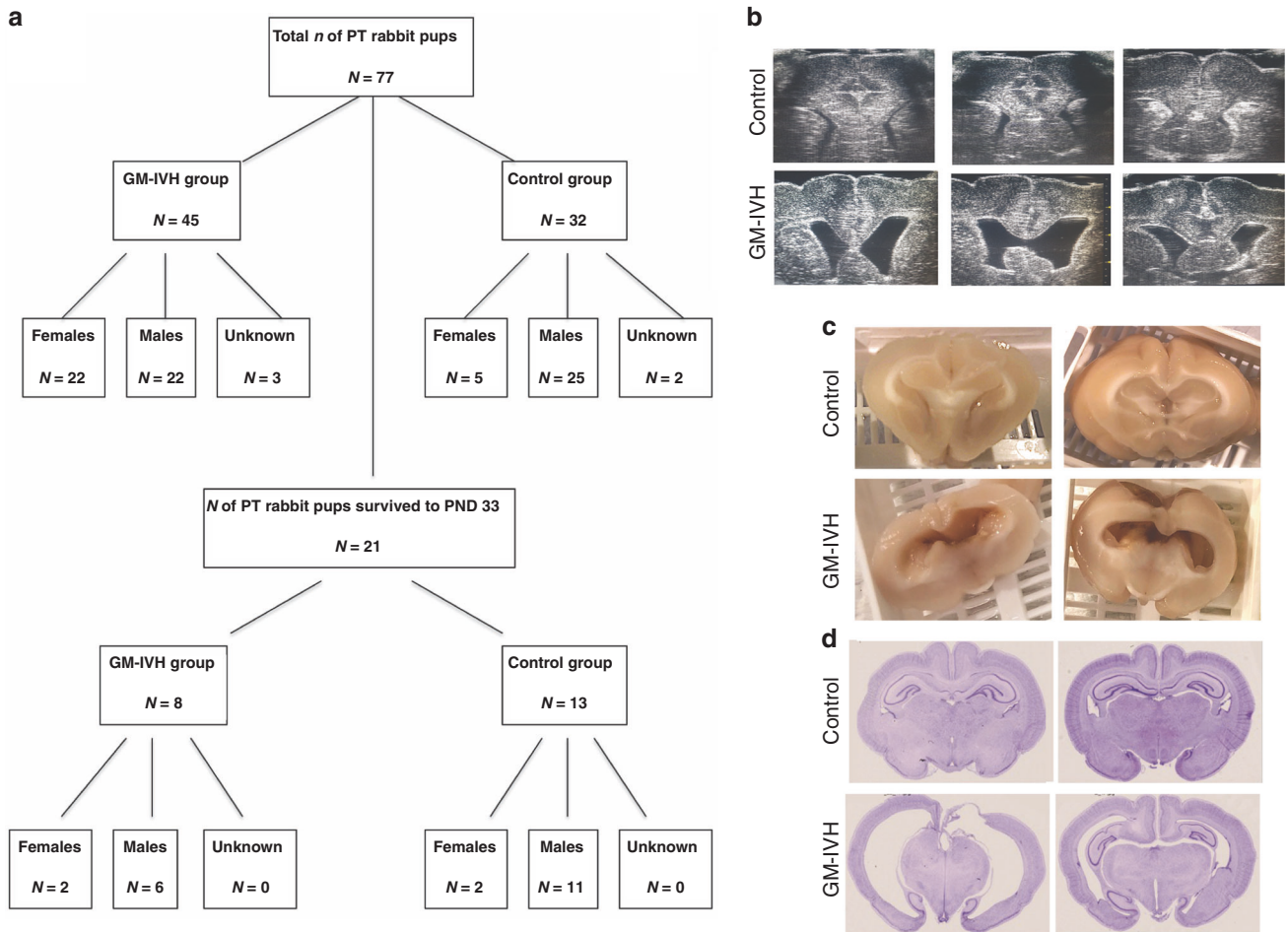


Fig. 1 Flow chart of the study and overall disturbance to brain structure. Number of rabbit pups in IVH with PHVD and control groups according to sex (a). The impact of IVH was visible via (b) high-frequency ultrasound ex vivo at PND33 in which coronal sections were obtained in a rostral-caudal direction; (c) at the macroscopic examination; and (d) with hematoxylin–eosin stains of coronal sections (scale bar = 25 mm).

inclined slope revealed no differences between the IVH and the control groups (mean (SD): 20.2 ± 11.2 s vs 21.5 ± 15.4 s, $p = 0.8$).

During the OF test with a duration of 5 min, both groups of preterm rabbits spent nearly half of the testing time in the peripheral zone with their body touching the wall (mean (SD) time was 141.5 ± 92 s vs 124.3 ± 93 s, for the IVH and control groups, respectively, $p = 0.7$). Entries into the central zone did not differ by groups as 4 IVH (53%) and 7 controls (53%) entered the central zone of the arena and there were no differences in the exploration time in the central zone between the groups (mean (SD) time was 10.4 ± 11 s vs 8 ± 16 s, for the IVH/PHVD and control groups, respectively, $p = 0.7$). There were no differences in global activity and in total covered distance between the IVH/PHVD group and control groups (mean (SD) distance was 332.16 ± 332.2 cm vs 219.1 ± 286.2 cm, respectively; $p = 0.5$). There was no difference in median latency time to escape from peripheral to the central zone between the groups, being a mean (SD) 64.3 ± 64.3 s vs 86.2 ± 96.0 s for the IVH and control groups, respectively; $p = 0.6$).

There were also no differences in the ORT test: both groups of animals exhibited comparable exploratory behavior with similar exploration times on 3 consecutive examination days. Both groups recognized the old and the new object in the 5-, 30- and 240-min interval without differences between the two groups (Table 2). Two animals (one for each group) were excluded from the ORT analysis: both animals froze at the starting point for the whole 5-min testing period.

IVH caused differences in myelin organization

The IVH group animals had a reduced density of myelin immunoreactivity (MBP staining) across the eight examined regions compared to the controls ($p = 0.002$, two-way ANOVA). This was revealed to be specifically apparent in the corona radiata compared to the controls in the post-test ($p = 0.011$; Fig. 3a). Furthermore, we analyzed the organization (directionality) of the MBP staining in the cortex and corpus callosum and observed significant effects of IVH ($p = 0.0146$, two-way ANOVA) that in the post-test were specifically apparent in the cortex ($p = 0.026$, Fig. 3b, c).

IVH reduces the numbers of mature neurons and synaptophysin area coverage and alters the development of the cortical layers

In the neuron density assessment, IVH pups had a lower number of neurons overall in the five assessed regions ($p = 0.008$, two-way ANOVA) compared to controls (Fig. 4a, b). In the post-test, this was specifically apparent in the thalamus ($p = 0.035$) compared to controls. Focusing specifically on the cortex, guided by layer-specific staining of adjacent sections (Fig. 4c–e) we noted that there was no effect on the numbers of mature neurons each in layers I–III, IV, and V–VI (Fig. 4e). The total cortical depth in the IVH rabbits was marginally smaller but not significantly different from that in the controls (mean \pm SEM) control, 1776.69 ± 245.39 , $n = 6$ vs IVH, 1674 ± 188.29 , $n = 6$). However, analysis of the width of each of the cortical layers, as a percentage of total cortical depth,

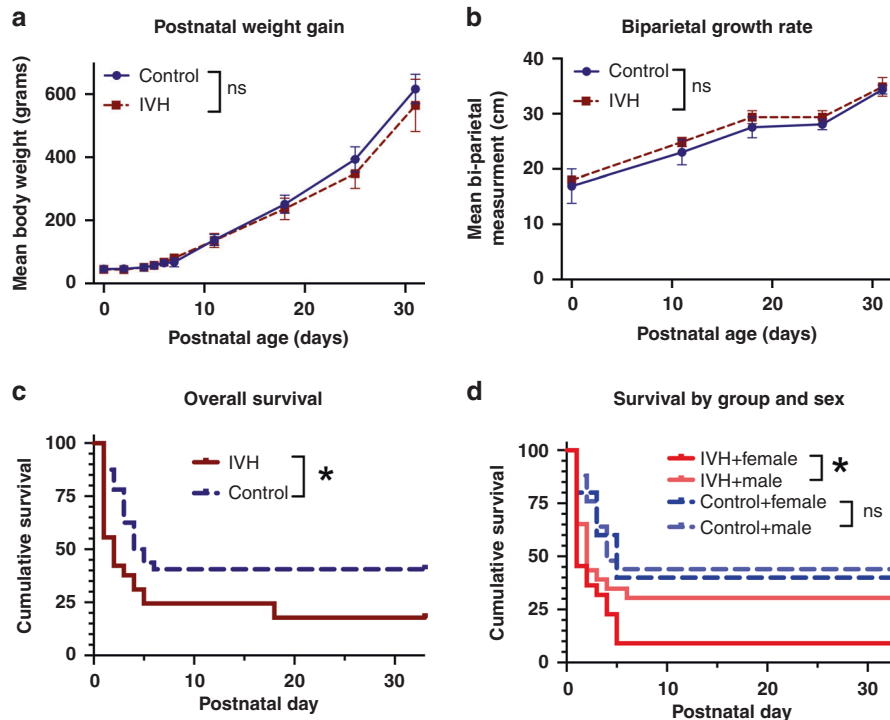


Fig. 2 Postnatal growth and survival of rabbit pups. There were no differences in somatic growth indices (**a**, **b**) between all pups with IVH and controls or when analyzed by sex (data not shown). IVH was associated with a significant decrease in pup survival (**c**). Survival in female preterm pups was close to a significantly lower level compared to male preterm pups ($p = 0.05$; **d**). Fewer female preterm pups with IVH survived until the study endpoint compared to the preterm male pups ($p = 0.015$; **d**). Data are shown as median \pm 95% CI, group differences evaluated with two-way ANOVA (**a**, **b**), and survival illustrated with Kaplan–Meier curves (**c**, **d**). Control, $n = 13$ (female = 2); IVH, $n = 8$ (female = 2); * $p < 0.05$.

revealed that there was an effect of IVH ($p = 0.0289$, two-way ANOVA, Fig. 4d). In the post-test, the depth of the upper cortical layers (I–III) was found to be significantly reduced in IVH brains compared to controls ($p = 0.044$; Fig. 4d). The IVH group animals also had a reduced density of presynaptic immunoreactivity (synaptophysin staining) across the six regions examined ($p = 0.003$, two-way ANOVA) compared to the controls (Fig. 4f, g).

IVH altered the number, distribution and maturation of interneurons

Cortical layer markers (CTIP2/NECAB) were used to demarcate the upper (I–III) and lower (IV–VI) layers (as per Fig. 4c) and adjacent sections were stained for PV and WF for the PNN. The number of PV-positive interneurons in the cortical layers was significantly altered by IVH ($p = 0.0244$, two-way ANOVA), and the post hoc test highlighted a significant reduction in PV-positive cell number in layer IV–VI ($p = 0.035$, Fig. 5a). We also determined the total numbers of cells that were PV-PNN positive (PNN+) interneurons and PV-PNN negative (PNN-) interneurons (Fig. 5b–d). There was a significant effect of IVH on the number of PNN expressing PV interneurons in the upper cortical region (I–III, $p = 0.0096$, two-way ANOVA) but in the post hoc no specific location change (Fig. 5c). There was also a significant effect of IVH on the number of PNN expressing PV interneurons in the lower cortical regions (IV–VI; $p = 0.0013$, two-way ANOVA). The post hoc specifically localized this to a reduction in the numbers of PV + PNN- cells ($p = 0.0073$, Fig. 5d).

IVH caused no change in GFAP but decreased the area coverage of IBA1

The number of GFAP-positive astrocytes did not significantly differ due to IVH, across the evaluated brain regions (nucleus caudate, thalamus, hypothalamus, hippocampus, or cortex) except the

internal capsule showing the significant reduction of GFAP-positive cells in IVH pups compared to the controls (two-way ANOVA, data not shown). The IVH group animals had a reduced density of IBA1 immunoreactivity (microglia/macrophage marker) across the eight regions examined ($p = 0.086$, two-way ANOVA) compared to the controls (Fig. 6a, b).

DISCUSSION

This is the first small animal study on the long-term effects of IVH (out to PND 30) with subsequent PHVD development in a preterm animal model. IVH caused persistent changes in cortical structure, neuronal number, synapse density, and myelin. However, we could not detect any alterations in the neurobehavioral assessment. Most studies previously undertaken in models of preterm rabbit IVH have been focused on short-term outcomes, predominantly terminating at PND14.^{20,21,27,35–48}

Survival in the preterm rabbit IVH model has previously not been described beyond PND14. However, in this study, most pup loss occurred during the first week of life, which agrees with previous findings.^{20,27,38} Compared to non-IVH preterm rabbit studies, we reported a lower overall survival within the first month of life (40% vs previous 56%.^{32,49}) Also, we observed a reduced survival in female pups in the IVH group that has not been previously reported for preterm non-IVH pups.^{31,49} Survival based on sex has not been reported previously in short-term studies in the preterm IVH rabbit pup model. In human infants, it is male sex that is associated with higher mortality and major morbidity.⁵⁰ Unfortunately, due to the high mortality in female pups, we could not undertake sex-specific analysis in this study, but we observed no difference in somatic growth indices. Importantly, using this data future studies will be powered to enable the capture of sex-related differences in outcome.

Table 2. Exploration times and novel object recognition ratios in the ORT.

| Exploration time (min) | GM-IVH (N = 7) | | | | | | | Control (N = 12) | | | | | | | | | |
|---------------------------------|---------------------------------------|------|------|------|--------|------|------|--------------------------------|------|-----|-----|------|--------|------|------|---------|--|
| | Mean | SD | Min | Max | Median | 25th | 75th | p value | Mean | SD | Min | Max | Median | 25th | 75th | p value | |
| Exploration time (min) | | | | | | | | | | | | | | | | | |
| 5 min (s) | 19.1 | 14.3 | 6.5 | 47.4 | 11.1 | 9.6 | 24.1 | 0.021 | 13.1 | 8.9 | 0 | 34.2 | 11.6 | 8.0 | 17.3 | 0.028 | |
| 240 min (s) | 15.1 | 9.9 | 1.95 | 32.2 | 12.1 | 9.1 | 21.9 | 0.028 | 17.8 | 5.7 | 7.7 | 27.6 | 17.4 | 14.3 | 22.9 | 0.002 | |
| Novel object recognition ratios | | | | | | | | | | | | | | | | | |
| 5 min | 0.47 (−0.07; 0.91) 0.35 (−0.27; 0.84) | | | | | | | 0.56 (−1; 1) 0.52 (0.16; 0.87) | | | | | | | | | |
| 240 min | | | | | | | | | | | | | | | | | |

Data for novel object recognition ratios are displayed as median with interquartile ranges.

Our study is the first to apply rearing by a wet nurse in the preterm rabbit pup IVH model instead of gavage feeding. A wet nurse avoids the mechanical trauma caused by repeated insertion of the feeding tube, as well as stress and hypothermia and has previously been described in a preterm rabbit model of fetal growth restriction.⁵¹ The importance of breastfeeding in rabbit pups was emphasized in a recent study, where term pups reared by does display improved social interactions when compared to term-born gavage reared pups.⁵² Olfactory cues from lactating rabbit does are involved in breathing stimulation, distress response alleviation, attention, and directional response stimulation and may promote learning and social behavior.^{53,54}

We undertook neurobehavioral testing in this study, because for children who develop PHVD, motor, co-ordination, and neurocognitive issues are frequent and do not decline with increasing age.^{9–14} Ours is the first study to evaluate neurobehavioral assessment at PND30. Previous work with this model at PND1–3 and PND14 demonstrated that pups with IVH have impaired neurobehaviour,^{20,35,36,41,42,45–47} including impaired motor functions and altered gait ability at P3²⁷ and PND14.^{20,35,36,41,42,45–47} At this extended time point (P30), we were unable to detect any differences in motor, gait, coordination, or for global motor activity and exploration as an indicator of anxiety levels. We speculate that this absence of neurobehavioral deficit may stem from advanced recovery in the pup, which is also often observed after early-life injury in the rodent,¹⁷ combined with the additional positive impacts of the wet nurse on development, described above.^{52–54} That said, we performed the ORT, using a paradigm similar to that previously validated by us^{30,31} to induce learning in preterm rabbits raised by wet nurse (as for this study). Thus, the lack of clear effects on motor, coordination and neurocognitive functions may be related to a strong compensatory capacity of the animals with the later testing time point (compared to previous studies) and maturation per se. We also cannot exclude that with increasing age neurobehavioral injury may manifest and longer-term follow-up is also warranted. Altogether, further optimization of behavioral paradigms should be explored in rabbits to strengthen the utility of this model.

Oligodendrocyte maturational arrest and hypomyelination is a hallmark of brain injury associated with preterm birth in infants.^{55,56} We observed a global reduction in the area coverage for myelin caused by IVH, supporting several short-term studies showing disruption of oligodendrocyte maturation and the myelination process in the preterm rabbit IVH model.^{20,35,36,41,45,46} Myelination in term rabbit pups initiates at around PND4²⁰ and reaches its peak at around PND18, with a delayed but more rapid increase in the myelination of fiber tracts in the internal capsule compared to the corpus callosum.⁵⁷ Changes in myelination quantity and also structure is considered to be responsible for long-term neurological sequela in human infants⁵⁸ and IHV led to altered myelin fiber orientation in an analysis relatively sensitive to subtle changes in MBP organization.⁵⁹

Along with WM damage in children and adults who developed IVH, recent research has focused on gray matter (GM) damage. Alterations in thalamocortical networks and reduced GM volume are associated with adverse cognitive outcomes and behavioral disorders in IVH compared to controls.^{60–62} The results of our study showed a collection of subtle neuronal deficits, including that preterm rabbit pups with IVH had a global reduction in mature neuronal number, altered cortical layering, and an interneuronopathy. Recent data from Dohare et al. showed a significant reduction of SAT2B and CUX1 expressing neurons in the upper cortical layer (II–IV) in preterm IVH pups at PND14⁴⁷ supporting our data of upper cortical layer thinning. However, with our count of total cell numbers we were unable to detect any differences in total neuronal number, despite the region being significantly thinner. Furthermore, preterm rabbits with IVH/PHVD had a reduced number of neurons in the nucleus caudate and

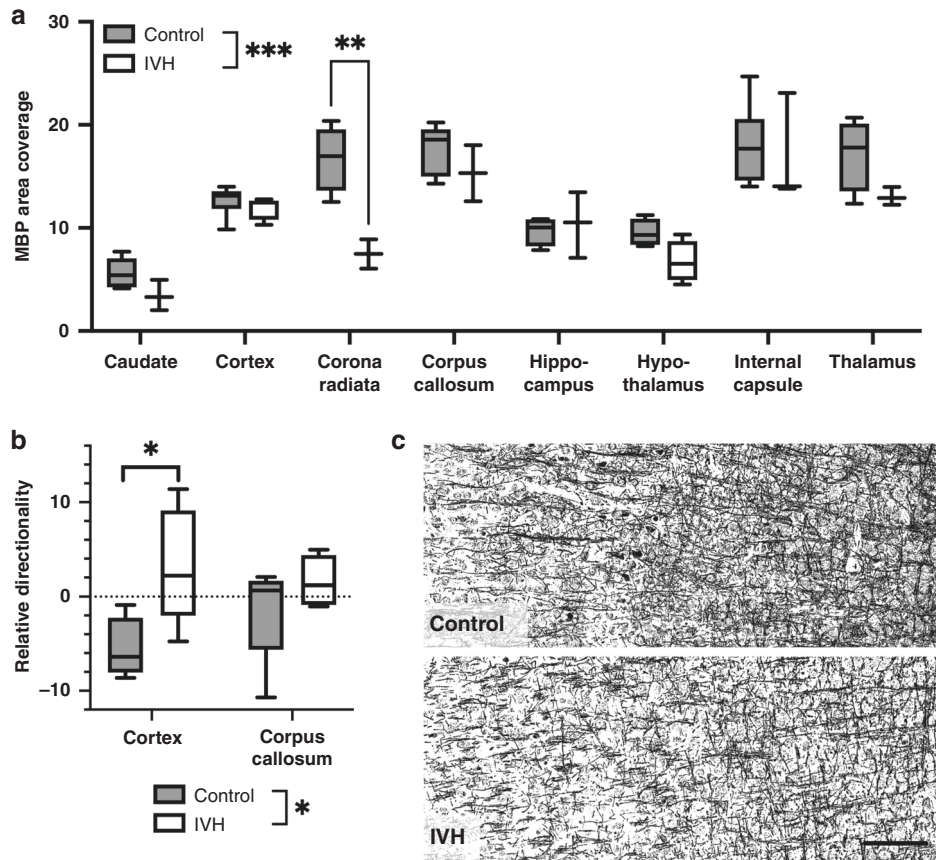


Fig. 3 Myelin area coverage and organization were significantly altered in pups with IVH and PHVD. Pups with IVH and PHVD had a reduction of MBP area as compared to controls (a) and an altered organization of MBP stained fibers (b) as shown in the representative photomicrographs of the cortical MBP staining in (c) (scale bar = 20 μ M). Data shown are median \pm 95% CI. Control, $n = 6$, IVH, $n = 6$. Evaluated with two-way ANOVA, * $p < 0.05$; ** $p < 0.01$; *** $p < 0.001$.

thalamus, highlighting the involvement of GM in the pathogenesis of IVH/PHVD. Reduced neurogenesis in the thalamus and nucleus caudate has been reported in several preterm human post mortem studies,^{63,64} as well as in different animal models of neonatal brain injury.^{65–67}

The effect of IVH on cortical PV interneurons in the preterm rabbit pup was assessed for the first time in our study. Cortical interneuron populations are vulnerable in preterm infants as they are still undergoing migration and maturation at the time of preterm birth.⁶⁸ Specifically, IVH/PHVD group animals had a lower number of PV-positive PNN-negative interneurons in the deep layers. In agreement, studies evaluating injury related to preterm birth and inflammation³³ and hypoxia–ischemia⁶⁹ have reported fewer PNN-positive interneurons. The PNN is a key regulator of perisomatic input to PV interneurons and thus overall network activity, meaning that tight regulation of the PNN is needed for typical brain function.⁷⁰ It might be that IVH/PHVD disrupts the maturation of PV-positive interneurons possibly due to the damage of the choroid plexus, where homeobox protein orthodenticle homeobox-2 (Otx2), involved in the expression of PNN, is released.

IVH also significantly reduced synaptophysin, a pre-synaptic terminal marker, supported by similar observations in a guinea pig model of intrauterine growth restriction (IUGR),⁷¹ a rat model of IUGR,⁷² and by observations of synaptic degradation in human cases of hydrocephalus.⁷³ Very little is known about the pattern of synaptogenesis in the rabbit, except a single study of the retina indicating that synaptogenesis occurs from PND9, reaching a plateau at PND20.⁷⁴ The decreased expression of synaptophysin may reflect disrupted synaptogenesis including altered processes

of synaptic remodeling by microglia. Synaptic pruning is a key function of microglia during the later stages of brain development,^{75,76} such that depleting microglia can change the structural connectome of the developing mouse brain.⁷⁷ We observed a reduction in the area coverage of IBA1, likely a loss of complexity due to ongoing inflammatory activation. We have made similar reports previously in a model of preterm brain injury in the mouse⁷⁸ and these kinds of region-specific subtle changes has also been reported in a model of IUGR in the piglet.⁷⁹ That there was a change in morphology was qualitatively supported when observing the stained sections, as the cell processes were less elaborate.

Our model of IVH in preterm rabbit pups carries a high translational value to the human situation, as it reflects a true preterm scenario, with the pups having underdeveloped lungs and gut, and being deprived of placentally derived trophic factors. This is reflected in the fact that preterm birth alone in this model induces brain injury reminiscent of that seen in preterm born infants.^{26,49}

All pups in our study received glycerol and we did not include “sham” control animals to evaluate of the effects of glycerol. We used this experimental design because: (1) renal function tests to define the glycerol toxicity in this model found them to be within normal limits, except for a slight increase in blood urea nitrogen,²⁷ (2) there is no evidence of inflammation, cell death, or neuronal degeneration in the forebrain of animals treated with glycerol without IVH vs the pups without glycerol treatment,²⁷ and (3) glycerol is widely used clinically, both in adult and pediatric populations, to treat brain edema and increased intracranial pressure^{80,81} with no reported changes in brain levels

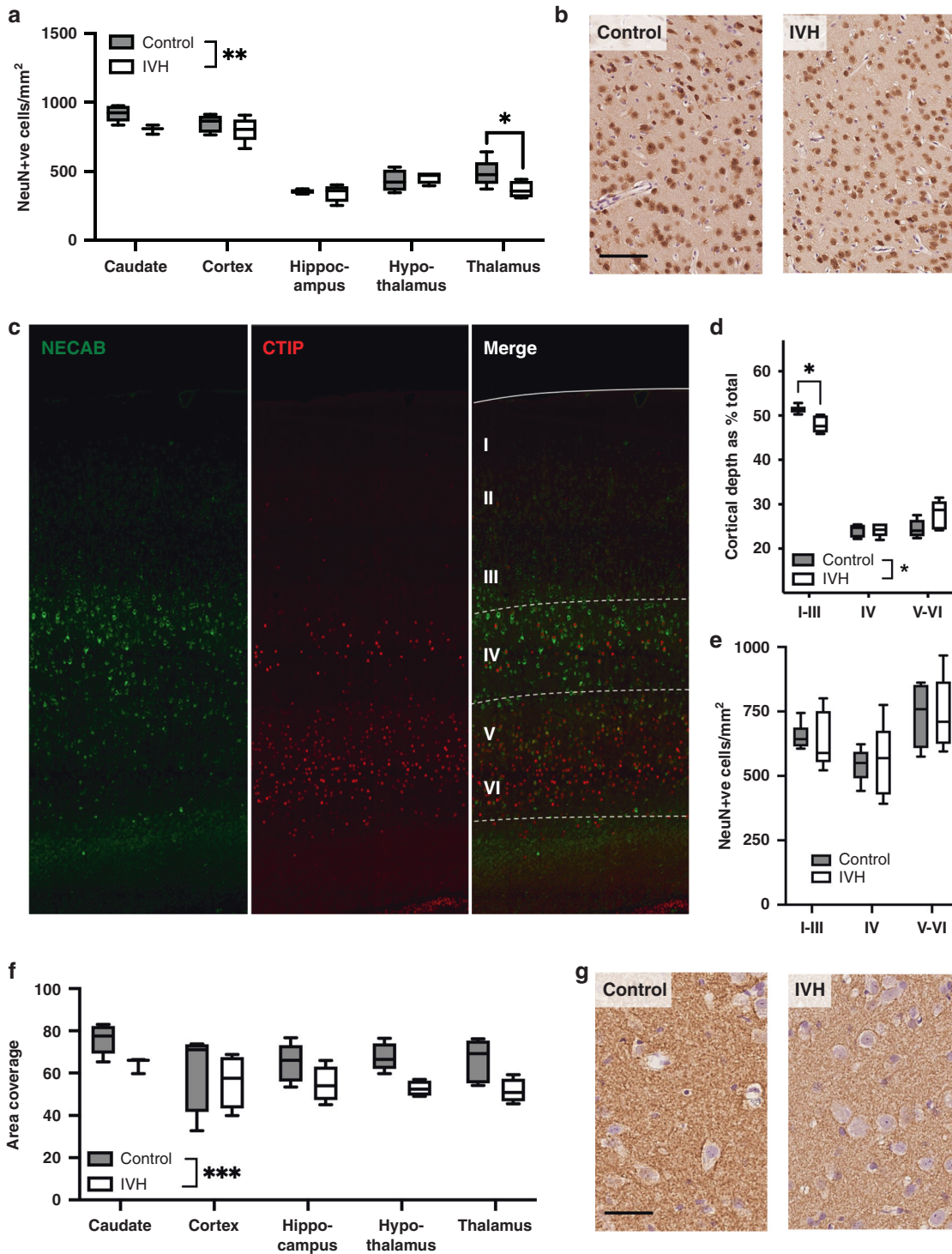


Fig. 4 NeuN-positive cell number and synaptophysin coverage is reduced and cortical organization altered in pups with IVH. Pups with IVH had a reduced number of NeuN-positive cells as compared to controls (a) shown in a representative micrograph of the thalamus (b) (scale bar = 100 μ M). Cortical layers were demarcated using staining for CTIP2 and NECAP and compared between pups with IVH and controls (c). There was a reduction in the depth of layers I-III (d) but no layer-specific change in the total number of NeuN-positive cells in the cortical layers (e). Pups with IVH had a reduction in synaptophysin-positive staining area as compared to controls (f) shown in a representative photomicrograph from the thalamus in (g) (scale bar = 25 μ M). Data shown are median \pm 95% CI. Evaluated with a two-way ANOVA and Sidak post hoc test. Control, $n = 6$, IVH, $n = 6$. * $p < 0.05$; ** $p < 0.01$; *** $p < 0.001$.

glutamate, pyruvate, and lactate in people injected with glycerol.⁸¹ However, the use of glycerol injected controls ensure that any biochemical effects of this osmotic agent are controlled for in both groups.

Inherent high mortality in this model led to small sample sizes and reduced power for the detection of significant differences between groups and a sex-specific analysis. Although we wish to mention that the apparent increased vulnerability of females in this

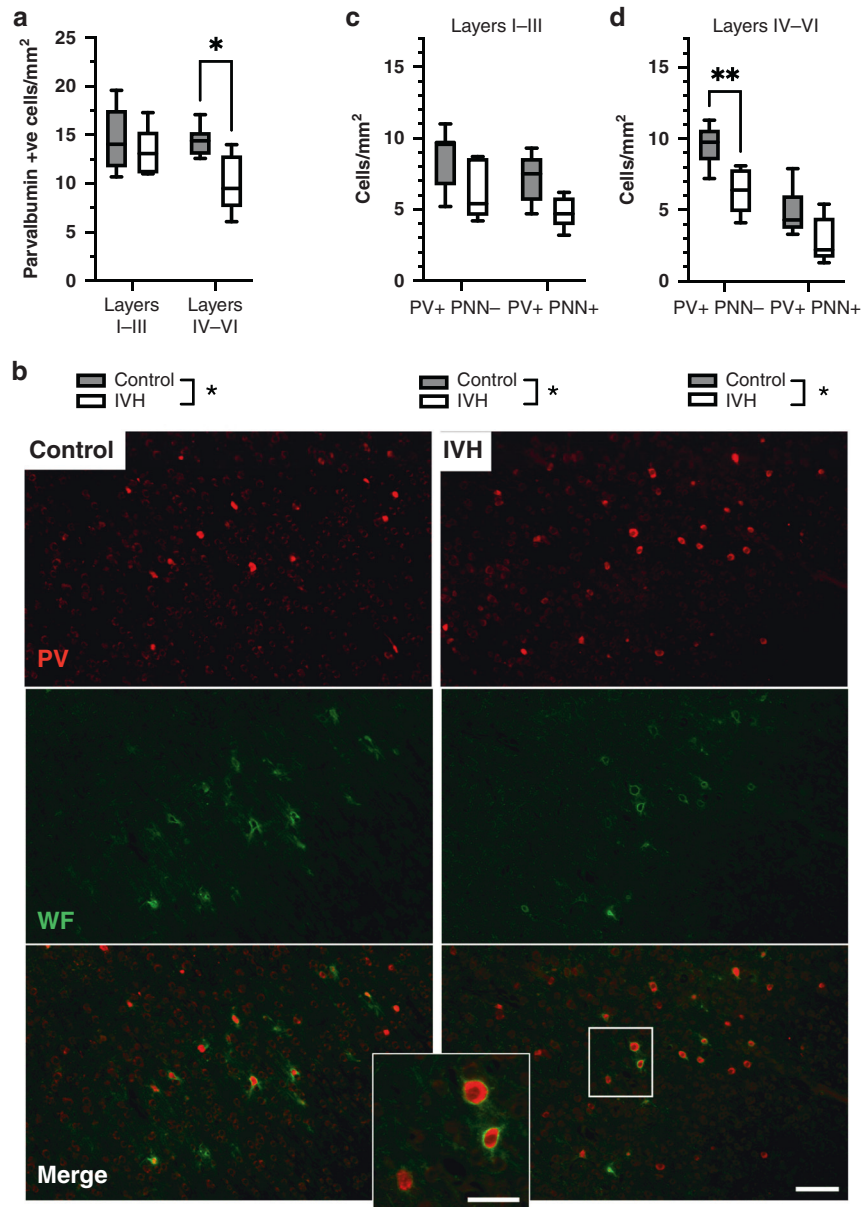


Fig. 5 Interneuron development is altered in pups with IVH and PHVD. In pups with IVH vs controls, there was a reduction in the numbers of PV-positive interneurons in the lower cortical layers (IV–VI) (a) and there was a specific reduction in the PV-positive cells not co-positive for the perineuronal net (PNN) protein (b). There was no difference in PV-positive cells with or without PNN in the upper layers (layers I–III) (c), again in the lower cortical regions only as shown in d. Data shown are median \pm 95% CI. Control vs IVH evaluated with two-way ANOVA. Control, $n = 6$, IVH, $n = 6$. * $p < 0.05$. ** $p < 0.01$. (Scale bar = low magnification 100 μm , high magnification inset = 50 μm).

paradigm is in contrast to the typical “male disadvantage” reported for perinatal brain injuries.^{82,83} Ours is the very first data on sex-based survival reported in the glycerol-induced IVH model and many rabbit studies in other paradigms have not reported sex or there have been no differences in outcomes.^{84–86} However, one study of the impacts of preterm birth on rabbit brain delivery has reported that, compared with females, males have less damage in the hippocampus (assessed via fractional anisotropy) and greater numbers of neurons in the caudate nucleus (NeuN-positive cell number).⁴⁹

There may also be a selection effect, introduced by the “healthiest” preterm pups surviving to the study endpoint while the pups with severe damage dying during the neonatal period masks possible differences potentially present in the original

sample size. This is an unavoidable phenomenon, also occurring in long-term follow-up studies of infants where early mortality is greatest for infants with the most severe IVH.

This study introduces important information for the field. For the first time, we report the long-term effects of IVH leading to PHVD in a preterm animal model that include alterations to myelination, including organizational changes, decreased mature neuron and presynaptic terminal densities, altered cortical organization, and altered PV-positive interneurons number and maturation. The lack of corresponding behavioral deficits may reflect the need for improved behavioral testing paradigms in this translationally valuable IVH model. These fundamental findings are important for furthering our understanding of mechanisms leading to WM and GM damage ultimately causing neurodevelopmental impairment in infants.

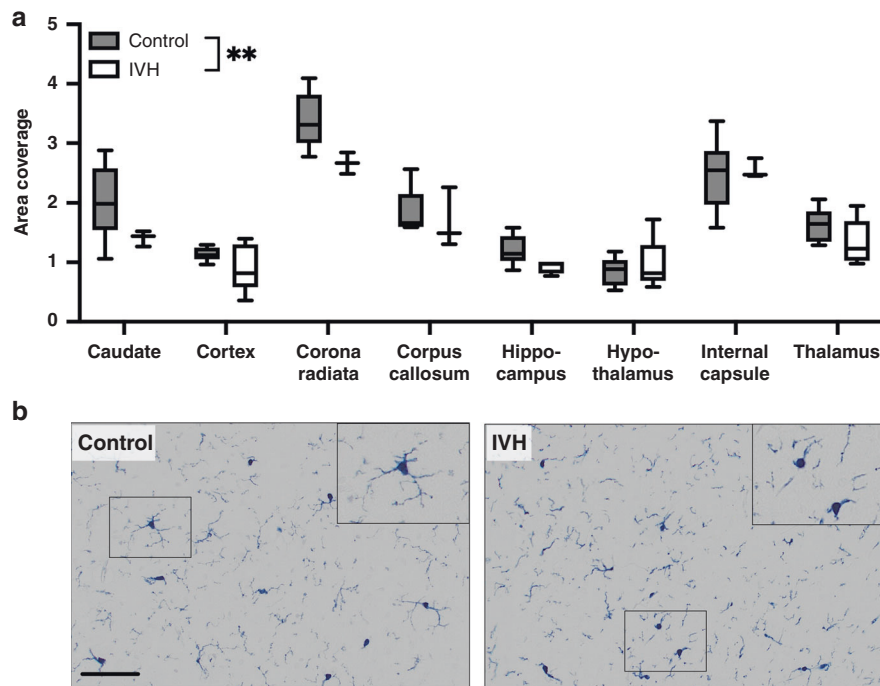


Fig. 6 IBA1 area coverage was significantly decreased in pups with IVH. Pups with IVH had a reduction of IBA1 area coverage as compared to controls **a** as shown in representative photomicrographs of the cortical MBP staining in **b** (scale bar = 100 μm). Data shown are median ± 95% CI. Control, $n = 6$, IVH, $n = 6$. Evaluated with two-way ANOVA, $**p < 0.01$.

DATA AVAILABILITY

The datasets generated during and/or analyzed during the current study are available from the corresponding author on reasonable request.

REFERENCES

- Ahn, S. Y., Shim, S. Y. & Sung, I. K. Intraventricular hemorrhage and post hemorrhagic hydrocephalus among very-low-birth-weight infants in Korea. *J. Korean Med. Sci.* **30**(Suppl 1), S52–S58 (2015).
- Szpecht, D., Nowak, I., Kwiatkowska, P., Szymankiewicz, M. & Gadzinowski, J. Intraventricular hemorrhage in neonates born from 23 to 26 weeks of gestation: retrospective analysis of risk factors. *Adv. Clin. Exp. Med.* **26**, 89–94 (2017).
- Yeo, K. T. et al. Improving incidence trends of severe intraventricular haemorrhages in preterm infants <32 weeks gestation: a cohort study. *Arch. Dis. Child. Fetal Neonatal Ed.* **105**, 145–150 (2020).
- Younge, N. et al. Survival and neurodevelopmental outcomes among periviable infants. *N. Engl. J. Med.* **376**, 617–628 (2017).
- Norman, M. et al. Association between year of birth and 1-year survival among extremely preterm infants in Sweden during 2004–2007 and 2014–2016. *JAMA* **321**, 1188–1199 (2019).
- Brouwer, A. et al. Neurodevelopmental outcome of preterm infants with severe intraventricular hemorrhage and therapy for post-hemorrhagic ventricular dilatation. *J. Pediatr.* **152**, 648–654 (2008).
- Stoll, B. J. et al. Trends in care practices, morbidity, and mortality of extremely preterm neonates, 1993–2012. *JAMA* **314**, 1039 (2015).
- Kim, J. K., Chang, Y. S., Sung, S. & Park, W. S. Mortality rate-dependent variations in the survival without major morbidities rate of extremely preterm infants. *Sci. Rep.* **9**, 7371 (2019).
- Adams-Chapman, I., Hansen, N. I., Stoll, B. J. & Higgins, R. & NICHD Research Network. Neurodevelopmental outcome of extremely low birth weight infants with posthemorrhagic hydrocephalus requiring shunt insertion. *Pediatrics* **121**, e1167–e1177 (2008).
- Whitelaw, A. et al. Randomized clinical trial of prevention of hydrocephalus after intraventricular hemorrhage in preterm infants: brain-washing versus tapping fluid. *Pediatrics* **119**, e1071–e1078 (2007).
- Bassan, H. et al. Timing of external ventricular drainage and neurodevelopmental outcome in preterm infants with posthemorrhagic hydrocephalus. *Eur. J. Paediatr. Neurol.* **16**, 662–670 (2012).
- Cizmeci, M. N. et al. Assessment of brain injury and brain volumes after post-hemorrhagic ventricular dilatation: a nested substudy of the randomized ELVIS trial. *J. Pediatr.* **208**, 191–197.e2 (2019).
- Luyt, K. et al. Drainage, irrigation and fibrinolytic therapy (DRIFT) for post-haemorrhagic ventricular dilatation: 10-year follow-up of a randomised controlled trial. *Arch. Dis. Child. Fetal Neonatal Ed.* **105**, 466–473 (2020).
- Shankaran, S. et al. Outcomes following post-hemorrhagic ventricular dilatation among infants of extremely low gestational age. *J. Pediatr.* **226**, 36–44.e3 (2020).
- Ryckman, K. K., Dagle, J. M., Kelsey, K., Momany, A. M. & Murray, J. C. Replication of genetic associations in the inflammation, complement and coagulation pathways with intraventricular hemorrhage in low birth weight preterm neonates. *Pediatr. Res.* **70**, 90–95 (2011).
- Villamor-Martinez, E. et al. Chorioamnionitis is a risk factor for intraventricular hemorrhage in preterm infants: a systematic review and meta-analysis. *Front. Physiol.* <https://doi.org/10.3389/fphys.2018.01253> (2018).
- Romantsik, O., Bruschetti, M. & Ley, D. Intraventricular hemorrhage and white matter injury in preclinical and clinical studies. *NeoReviews* **20**, e636–e652 (2019).
- Semple, B. D., Blomgren, K., Gimlin, K., Ferrero, D. M. & Noble-Haesslein, L. J. Brain development in rodents and humans: Identifying benchmarks of maturation and vulnerability to injury across species. *Prog. Neurobiol.* **106–107**, 1–16 (2013).
- Conner, E. S., Lorenzo, A. V., Welch, K. & Dorval, B. The role of intracranial hypotension in neonatal intraventricular hemorrhage. *J. Neurosurg.* **58**, 204–209 (1983).
- Chua, C. O. et al. Consequences of intraventricular hemorrhage in a rabbit pup model. *Stroke* **40**, 3369–3377 (2009).
- Sveinsdóttir, S., Cinthio, M. & Ley, D. High-frequency ultrasound in the evaluation of cerebral intraventricular haemorrhage in preterm rabbit pups. *Ultrasound Med. Biol.* **38**, 423–431 (2012).
- D’Angio, C. T. & Ryan, R. M. Animal models of bronchopulmonary dysplasia. The preterm and term rabbit models. *Am. J. Physiol. Lung Cell. Mol. Physiol.* **307**, L959–L969 (2014).
- Salaets, T. et al. Preterm birth impairs postnatal lung development in the neonatal rabbit model. *Respir. Res.* **21**, 59 (2020).
- Bozeman, A. P., Dassinger, M. S., Birusingh, R. J., Burford, J. M. & Smith, S. D. An animal model of necrotizing enterocolitis (NEC) in preterm rabbits. *Fetal Pediatr. Pathol.* **32**, 113–122 (2013).
- de Winter, D. et al. Glomerular developmental delay and proteinuria in the preterm neonatal rabbit. *PLoS ONE* **15**, e0241384 (2020).
- Sveinsdóttir, K. et al. Impaired cerebellar maturation, growth restriction, and circulating insulin-like growth factor 1 in preterm rabbit pups. *Dev. Neurosci.* **39**, 487–497 (2017).

27. Georgiadis, P. et al. Characterization of acute brain injuries and neurobehavioral profiles in a rabbit model of germinal matrix hemorrhage. *Stroke* **39**, 3378–3388 (2008).
28. Lorenzo, A. V., Welch, K. & Conner, S. Spontaneous germinal matrix and intraventricular hemorrhage in prematurely born rabbits. *J. Neurosurg.* **56**, 404–410 (1982).
29. Dutta, S. & Sengupta, P. Rabbits and men: relating their ages. *J. Basic Clin. Physiol. Pharmacol.* **29**, 427–435 (2018).
30. Gümüş, H. G. et al. Behavioral testing and litter effects in the rabbit. *Behav. Brain Res.* **353**, 236–241 (2018).
31. Van der Veecken, L. et al. Long-term neurological effects of neonatal caffeine treatment in a rabbit model of preterm birth. *Pediatr. Res.* **87**, 1011–1018 (2020).
32. van der Merwe, J. et al. Earlier preterm birth is associated with a worse neurocognitive outcome in a rabbit model. *PLoS ONE* **16**, e0246008 (2021).
33. Stolp, H. B. et al. Interneuron development is disrupted in preterm brains with diffuse white matter injury: observations in mouse and human. *Front. Physiol.* **10**, 955 (2019).
34. Sun, Y. et al. Sudan black B reduces autofluorescence in murine renal tissue. *Arch. Pathol. Lab. Med.* **135**, 1335–1342 (2011).
35. Vose, L. R. et al. Treatment with thyroxine restores myelination and clinical recovery after intraventricular hemorrhage. *J. Neurosci.* **33**, 17232–17246 (2013).
36. Vinukonda, G. et al. Intraventricular hemorrhage induces deposition of proteoglycans in premature rabbits, but their in vivo degradation with chondroitinase does not restore myelination, ventricle size and neurological recovery. *Exp. Neurol.* **247**, 630–644 (2013).
37. Gram, M. et al. Hemoglobin induces inflammation after preterm intraventricular hemorrhage by methemoglobin formation. *J. Neuroinflammation* **10**, 867 (2013).
38. Traudt, C. M., McPherson, R. J., Studholme, C., Millen, K. J. & Juul, S. E. Systemic glycerol decreases neonatal rabbit brain and cerebellar growth independent of intraventricular hemorrhage. *Pediatr. Res.* **75**, 389–394 (2014).
39. Sveinsdottir, S. et al. Altered expression of aquaporin 1 and 5 in the choroid plexus following preterm intraventricular hemorrhage. *Dev. Neurosci.* **36**, 542–551 (2014).
40. Gram, M. et al. Extracellular hemoglobin-mediator of inflammation and cell death in the choroid plexus following preterm intraventricular hemorrhage. *J. Neuroinflammation* **11**, 200 (2014).
41. Vinukonda, G. et al. Hyaluronidase and hyaluronan oligosaccharides promote neurological recovery after intraventricular hemorrhage. *J. Neurosci.* **36**, 872–889 (2016).
42. Vinukonda, G. et al. Human cord blood-derived unrestricted somatic stem cell infusion improves neurobehavioral outcome in a rabbit model of intraventricular hemorrhage. *Stem Cells Transl. Med.* **8**, 1157–1169 (2019).
43. Ley, D. et al. High presence of extracellular hemoglobin in the periventricular white matter following preterm intraventricular hemorrhage. *Front. Physiol.* **7**, 330 (2016).
44. Agyemang, A. A. et al. Cerebellar exposure to cell-free hemoglobin following preterm intraventricular hemorrhage: causal in cerebellar damage? *Transl. Stroke Res.* **8**, 461–473 (2017).
45. Dohare, P. et al. AMPA-kainate receptor inhibition promotes neurologic recovery in premature rabbits with intraventricular hemorrhage. *J. Neurosci.* **36**, 3363–3377 (2016).
46. Dohare, P. et al. Glycogen synthase kinase-3 β inhibition enhances myelination in preterm newborns with intraventricular hemorrhage, but not recombinant Wnt3A. *Neurobiol. Dis.* **118**, 22–39 (2018).
47. Dohare, P. et al. GSK3 β inhibition restores impaired neurogenesis in preterm neonates with intraventricular hemorrhage. *Cereb. Cortex* **29**, 3482–3495 (2019).
48. Romantsik, O. et al. The heme and radical scavenger α 1-microglobulin (A1M) confers early protection of the immature brain following preterm intraventricular hemorrhage. *J. Neuroinflammation* **16**, 122 (2019).
49. van der Merwe, J. et al. Early neuropathological and neurobehavioral consequences of preterm birth in a rabbit model. *Sci. Rep.* **9**, 3506 (2019).
50. Boghossian, N. S., Geraci, M., Edwards, E. M. & Horbar, J. D. Sex differences in mortality and morbidity of infants born at less than 30 weeks' gestation. *Pediatrics* **142**, e20182352 (2018).
51. Illa, M. et al. Long-term functional outcomes and correlation with regional brain connectivity by MRI diffusion tractography metrics in a near-term rabbit model of intrauterine growth restriction. *PLoS ONE* **8**, e76453 (2013).
52. Klebe, D. et al. Reduced hippocampal dendrite branching, spine density and neurocognitive function in premature rabbits, and reversal with estrogen or TrkB agonist treatment. *Cereb. Cortex* **29**, 4932–4947 (2019).
53. Schaal, B. et al. Mammary olfactory signalisation in females and odor processing in neonates: Ways evolved by rabbits and humans. *Behav. Brain Res.* **200**, 346–358 (2009).
54. Charra, R., Datiche, F., Gigot, V., Schaal, B. & Coureaud, G. Pheromone-induced odor learning modifies Fos expression in the newborn rabbit brain. *Behav. Brain Res.* **237**, 129–140 (2013).
55. Billiards, S. S. et al. Myelin abnormalities without oligodendrocyte loss in periventricular leukomalacia. *Brain Pathol. Zur. Switz.* **18**, 153–163 (2008).
56. Verney, C. et al. Microglial reaction in axonal crossroads is a hallmark of noncystic periventricular white matter injury in very preterm infants. *J. Neuropathol. Exp. Neurol.* **71**, 251–264 (2012).
57. Drobyshevsky, A., Jiang, R., Derrick, M., Luo, K. & Tan, S. Functional correlates of central white matter maturation in perinatal period in rabbits. *Exp. Neurol.* **261**, 76–86 (2014).
58. Hüppi, P. S. et al. Microstructural brain development after perinatal cerebral white matter injury assessed by diffusion tensor magnetic resonance imaging. *Pediatrics* **107**, 455–460 (2001).
59. van Tilborg, E. et al. A quantitative method for microstructural analysis of myelinated axons in the injured rodent brain. *Sci. Rep.* **7**, 16492 (2017).
60. Bjuland, K. J., Rimol, L. M., Løhaugen, G. C. C. & Skranes, J. Brain volumes and cognitive function in very-low-birth-weight (VLBW) young adults. *Eur. J. Paediatr. Neurol.* **18**, 578–590 (2014).
61. Bora, S., Pritchard, V. E., Chen, Z., Inder, T. E. & Woodward, L. J. Neonatal cerebral morphometry and later risk of persistent inattention/hyperactivity in children born very preterm. *J. Child Psychol. Psychiatry* **55**, 828–838 (2014).
62. Ball, G. et al. Thalamocortical connectivity predicts cognition in children born preterm. *Cereb. Cortex* **25**, 4310–4318 (2015).
63. Vontell, R. et al. Cellular mechanisms of Toll-like receptor-3 activation in the thalamus are associated with white matter injury in the developing brain. *J. Neuropathol. Exp. Neurol.* **74**, 13 (2015).
64. Panda, S. et al. Estrogen treatment reverses prematurity-induced disruption in cortical interneuron population. *J. Neurosci.* **38**, 7378–7391 (2018).
65. Dieni, S. et al. The pattern of cerebral injury in a primate model of preterm birth and neonatal intensive care. *J. Neuropathol. Exp. Neurol.* **63**, 1297–1309 (2004).
66. McClendon, E. et al. Prenatal cerebral ischemia triggers dysmaturation of caudate projection neurons. *Ann. Neurol.* **75**, 508–524 (2015).
67. Ardalan, M. et al. Dysmaturation of somatostatin interneurons following umbilical cord occlusion in preterm fetal sheep. *Front. Physiol.* **10**, 563 (2019).
68. Lim, L., Mi, D., Llorca, A. & Marín, O. Development and functional diversification of cortical interneurons. *Neuron* **100**, 294–313 (2018).
69. Fowke, T. M. et al. Loss of interneurons and disruption of perineuronal nets in the cerebral cortex following hypoxia-ischaemia in near-term fetal sheep. *Sci. Rep.* **8**, 17686 (2018).
70. Bozzelli, L. P., Alaiyed, S., Kim, E., Villapol, S. & Conant, K. Proteolytic remodeling of perineuronal nets: effects on synaptic plasticity and neuronal population dynamics. *Neural Plast.* **2018**, 1–13 (2018).
71. Piorkowska, K. et al. Synaptic development and neuronal myelination are altered with growth restriction in fetal guinea pigs. *Dev. Neurosci.* **36**, 465–476 (2014).
72. van de Looij, Y. et al. Nutritional intervention for developmental brain damage: effects of lactoferrin supplementation in hypocaloric induced intrauterine growth restriction rat pups. *Front. Endocrinol.* **10**, 46 (2019).
73. Castejón, O. Transmission electron microscope study of human hydrocephalic cerebral cortex. *J. Submicrosc. Cytol. Pathol.* **26**, 29–39 (1994).
74. McArdle, C. B., Dowling, J. E. & Masland, R. H. Development of outer segments and synapses in the rabbit retina. *J. Comp. Neurol.* **175**, 253–273 (1977).
75. Kettenmann, H., Kirchhoff, F. & Verkhratsky, A. Microglia: new roles for the synaptic stripper. *Neuron* **77**, 10–18 (2013).
76. Paolicelli, R. C. & Ferretti, M. T. Function and dysfunction of microglia during brain development: consequences for synapses and neural circuits. *Front. Synaptic Neurosci.* **9**, 9 (2017).
77. Paolicelli, R. C. et al. Synaptic pruning by microglia is necessary for normal brain development. *Science* **333**, 1456–1458 (2011).
78. Van Steenwinkel, J. et al. Decreased microglial Wnt/ β -catenin signalling drives microglial pro-inflammatory activation in the developing brain. *Brain* **142**, 3806–3833 (2019).
79. Wixey, J. A. et al. Neuropathology in intrauterine growth restricted newborn piglets is associated with glial activation and proinflammatory status in the brain. *J. Neuroinflammation* **16**, 5 (2019).
80. Righetti, E. et al. Glycerol for acute stroke: a Cochrane systematic review. *J. Neurol.* **249**, 445–451 (2002).
81. Berger, C., Sakowitz, O. W., Kiening, K. L. & Schwab, S. Neurochemical monitoring of glycerol therapy in patients with ischemic brain edema. *Stroke* **36**, e4–e6 (2005).
82. Charriat-Marlangue, C., Besson, V. C. & Baud, O. Sexually dimorphic outcomes after neonatal stroke and hypoxia-ischemia. *Int. J. Mol. Sci.* **19**, 61 (2018).
83. Tioseco, J. A., Aly, H., Essers, J., Patel, K. & El-Mohandes, A. A. E. Male sex and intraventricular hemorrhage. *Pediatr. Crit. Care Med.* **7**, 40–44 (2006).

84. Zhang, Z., Saraswati, M., Koehler, R. C., Robertson, C. & Kannan, S. A new rabbit model of pediatric traumatic brain injury. *J. Neurotrauma* **32**, 1369–1379 (2015).
85. Zhang, Z. et al. Cerebellar injury and impaired function in a rabbit model of maternal inflammation induced neonatal brain injury. *Behav. Anal. Anim. Models Intellect. Dev. Disabil.* **165**, 106901 (2019).
86. Zhang, Z. et al. Pediatric traumatic brain injury causes long-term deficits in adult hippocampal neurogenesis and cognition. *J. Neurotrauma* **37**, 1656–1667 (2020).

ACKNOWLEDGEMENTS

We wish to acknowledge Helena Karlsson, Claes Ekström, Christina Elvén, and Lise-Lotte Kuré, ImaGene-iT AB, Lund University for excellent technical assistance.

AUTHOR CONTRIBUTIONS

Each contributor made a substantial contribution to conception and design, acquisition of data, or analysis and interpretation of data, drafting the article or revising it critically for important intellectual content, and gave final approval of the version to be published.

FUNDING

The Swedish Research Council and governmental ALF research grants to Lund University supported this work. B.F.'s research and the PhD stipend of E.R.-M. were supported by the Cerebral Palsy Alliance (Australia). Open Access funding enabled and organized by CAUL and its Member Institutions.

COMPETING INTERESTS

The authors declare no competing interests.

ADDITIONAL INFORMATION

Supplementary information The online version contains supplementary material available at <https://doi.org/10.1038/s41390-022-02075-y>.

Correspondence and requests for materials should be addressed to Olga Romantsik or Bobbi Fleiss.

Reprints and permission information is available at <http://www.nature.com/reprints>

Publisher's note Springer Nature remains neutral with regard to jurisdictional claims in published maps and institutional affiliations.



Open Access This article is licensed under a Creative Commons Attribution 4.0 International License, which permits use, sharing, adaptation, distribution and reproduction in any medium or format, as long as you give appropriate credit to the original author(s) and the source, provide a link to the Creative Commons license, and indicate if changes were made. The images or other third party material in this article are included in the article's Creative Commons license, unless indicated otherwise in a credit line to the material. If material is not included in the article's Creative Commons license and your intended use is not permitted by statutory regulation or exceeds the permitted use, you will need to obtain permission directly from the copyright holder. To view a copy of this license, visit <http://creativecommons.org/licenses/by/4.0/>.

© The Author(s) 2022